

Improved two-temperature model with correction of non-Boltzmann effect for oxygen and nitrogen

Rui Xiong , Yufeng Han , and Wei Cao **High-Speed Aerodynamics Laboratory, Tianjin University, Tianjin 300072, China*

(Received 27 March 2024; accepted 10 July 2024; published 5 August 2024)

In thermochemical nonequilibrium processes, both the nonequilibrium between different kinds of internal energy of molecules and the non-Boltzmann (NB) energy state distribution significantly impact the dissociation rate coefficients. The conventional two-temperature (2-T) model fails to accurately portray these effects, especially the NB effect. Consequently, dissociation rate coefficients calculated by the 2-T model are inaccurate in simulating strong thermochemical nonequilibrium flow, resulting in a surface heat flux inconsistent with experimental data. This article investigates the influencing factor of the NB effect on the dissociation rate coefficient using the state-to-state (STS) method during the zero-dimensional heating process of N_2 and O_2 . Based on this, we develop a fitting formula to precisely correct the NB effect. Furthermore, we propose an improved model by integrating this fitting formula with the single-group linear maximum entropy model, which considers only the effect of nonequilibrium between different kinds of internal energy. This improved model provides an accurate description of thermochemical nonequilibrium on the dissociation rate coefficients. To validate the effectiveness of the improved model, we simulate the nonequilibrium process following a normal shock. The results demonstrate that in strong thermochemical nonequilibrium flow, compared to the 2-T Park model, the maximum and average discrepancies between the translation temperatures calculated by the improved model and those by the STS method are reduced by more than 68% and 82%, respectively. Additionally, the results closely align with experimental data, indicating that the improved model can accurately depict the effect of thermal nonequilibrium on dissociation rate coefficients.

DOI: [10.1103/PhysRevFluids.9.083201](https://doi.org/10.1103/PhysRevFluids.9.083201)

I. INTRODUCTION

As the speed of a hypersonic vehicle increases, the fluid temperature postshock and at the vehicle's surface rises. This phenomenon accentuates the challenge of surface heat protection for the vehicle. In addition to the rapid temperature increase, the strong bow shock at the head of a hypersonic vehicle also causes a sharp rise in pressure and the excitation of the internal energy of molecules behind the shock. These extreme conditions result in thermal and chemical nonequilibrium, leading to processes such as dissociation, ionization, and transitions within the fluid. The timescale of these processes is comparable to that of the flow itself, resulting in a flow in thermochemical nonequilibrium [1,2]. In this state, chemical reactions and the relaxation of internal energy significantly impact the fluid temperature and, consequently, the surface heat flux of the vehicle. Therefore, accurately simulating thermochemical nonequilibrium flow is crucial for precise calculation of the vehicle's surface heat flux and improvement of the thermal protection system design [3].

*Contact author: caow@tju.edu.cn

Internal energy relaxation and chemical reactions are key elements in the thermochemical nonequilibrium process, and both of them are influenced by various factors, including the energy of different internal energy modes and the nonequilibrium distribution of internal energy states, known as the non-Boltzmann (NB) effect. Therefore, it is challenging to accurately characterize the rates of these processes solely using temperature T , which represents the total internal energy, and thermochemical nonequilibrium models containing the above factors are necessary.

At present, two-temperature (2-T) models are widely employed to describe thermochemical nonequilibrium flow. These models utilize the Landau-Teller (L-T) theory [4] to characterize internal energy relaxation. The L-T theory defines relaxation based on the difference between specific vibrational energy and its equilibrium value, along with the characteristic relaxation time τ . In terms of chemical reactions, both chemical reaction rate coefficients and the change in vibrational energy during the chemical reaction are influenced by the thermochemical nonequilibrium effect, and the former exerts a more significant influence on the flow. As the recombination rate coefficient is unrelated to molecular thermal nonequilibrium, obtaining accurate dissociation rate coefficients becomes crucial for characterizing thermochemical nonequilibrium flows. 2-T models assume that the reaction rate in thermochemical nonequilibrium flow is determined by translational and vibrational energy, represented by translational temperature (T_{tr}) and vibrational temperature (T_v), respectively. To describe aforementioned effect, various 2-T models with different modifications have been developed based on theoretical analysis and experimental data. Widely used 2-T models include Park [5], Marrone-Treanor [6,7], Hansen [8], Macheret-Fridman [9,10], and others [11,12].

2-T models primarily focus on the nonequilibrium between translational and vibrational energy, assuming the energy state distribution is in equilibrium and inadequately describing the NB effect. As vehicle velocities increase, the degree of thermochemical nonequilibrium intensifies, leading to a strong NB distribution of energy states [13–15]. Moreover, the significant preferential dissociation of high-energy molecules greatly influences the NB distribution in the nonequilibrium process [16]. At the same time, the atoms produced by dissociation affect the degree of NB distribution of high-energy molecules by influencing the internal energy relaxation and dissociation rates within the system [17], making the impact of NB effects in the system more complex. Consequently, current research indicates that in flow simulations, ranging from simple flows after a normal shock to complex flows around a double wedge, the NB effect has a pronounced impact on the dissociation rate. Existing 2-T models struggle to accurately simulate strong thermochemical nonequilibrium flows [18–22]. Therefore, a more advanced approach is essential to properly depict the influence of the NB effect and accurately simulate chemical reactions and vibrational energy changes in strong thermochemical nonequilibrium flows.

The state-to-state (STS) approach [23–28] is a methodology that treats molecules at different energy states as distinct species, enabling a direct representation of reaction processes and avoiding inaccuracies induced by model assumptions. The STS method has proven successful in simulating many simple flows [29–32], significantly contributing to the investigation and interpretation of thermochemical nonequilibrium flow. Recently, the STS method has been further applied in simulations involving complex shapes [20,33].

However, current computational resources cannot afford large-scale simulations using the STS approach. Therefore, the 2-T model improved by simulated data from the STS approach and the reduced-order STS model are crucial solutions to enhance the accuracy of thermochemical nonequilibrium flow simulations. The maximum entropy model [34–37] partitions molecules into several groups while preserving the total internal energy and mass of each group during the flow iterative process. In the calculation of the reaction source term, the maximum entropy criterion is applied to reconstruct the complete energy state distribution. This allows for accurate reproduction of the calculation results obtained from the state-to-state (STS) method. The maximum entropy model still presents computational challenges, which arise not only due to the large number of reactions involved but also due to the stiffness problem caused by the small total mass and total energy of the high-energy group. Among the maximum entropy models, the single-group linear maximum

entropy [38,39] (SGLME) model assumes that molecules of each energy state are considered as one group and reconstructed by the linear maximum entropy criterion, implying that the molecules are under Boltzmann distribution. We pay attention to this model because, although it ignores the NB effect, it can completely reflect the influence of nonequilibrium of the internal energy modes on the dissociation rate. This feature is helpful for investigating the two types of thermal nonequilibrium effects individually and does not have the stiffness problem brought by the independent grouping of the high-energy states. Josyula [40,41] introduced a depletion model to capture the impact of the underdistribution of high-energy states on the dissociation rate. Nevertheless, this model falls short in representing the influence of the reaction history on the energy state distribution, leading to discrepancies when compared to the results obtained from the STS method. Colonna [38] proposed the two-level distribution (TLD) model. This model calculates the dissociation rate using the number density of molecules at the highest vibrational energy state and T_v . The model demonstrates effective correction under certain flow conditions but inadequately portrays the NB effects in simulating nozzle expansion flow, indicating a need for improvement. Neitzel [18] developed a two-temperature nonequilibrium non-Boltzmann (2T-NENB) model for the O_2 postshock process that utilizes an extra characteristic temperature to describe the NB effect. This model performs well in postshock simulations but fails to show significant improvement in double-cone flow simulations. Singh and Schwartztruber [42,43] proposed a model containing molecular properties that reconstruct energy state distributions in nonequilibrium processes and obtain the reaction rates more accurately, but this model needs further validation in complex flows. Mankodi and Myong [44] proposed the nonequilibrium total temperature (NETT) and nonequilibrium piecewise interpolation (NEPI) models. The former defines the dissociation rate based on a total temperature weighted according to the degrees of freedom and the deviation ratio β defined in terms of the internal energy temperature, while the latter uses an interpolation formula based on T_v segmentation to obtain the dissociation rate. These two models do not consider the influence of flow history on dissociation. Thus, they outperform in some cases but underperform in others. Chaudhry [45] proposed the modified Marrone-Treanor (MMT) model, which improved the parameters of the Marrone-Treanor model by the reaction rates calculated by the quasiclassical trajectory method [46]. Moreover, the NB effect on dissociation rate and vibrational energy loss per dissociation is corrected to obtain the MMT-NB [47,48] model, which successfully acquired better simulation results than conventional models. Further, data-driven approaches have also been applied to solve high-fidelity thermochemical nonequilibrium flow simulation problems [49]. However, current NB corrections are still not precise enough.

This study aims to develop an improved model that comprehensively considers the NB effect. To achieve this, the variation patterns of the NB effect with the equilibrium dissociation degree and the chemical reaction process are analyzed and summarized under zero-dimensional (0D) adiabatic conditions. Subsequently, a fitting expression for the correction factor of the NB effect is obtained, and a comparison is made between the fitting equation and the actual correction factor calculated during simulations. Furthermore, an improved model that accounts for the NB effect is proposed by integrating the NB factor with the SGLME model, which considers only the nonequilibrium of different internal energy modes. The improved model accurately captures the influence of thermal nonequilibrium on dissociation rates. To assess its performance, the improved model is compared with simulation results from the Park model and the STS method in the relaxation process simulation after one-dimensional (1D) postshock.

II. THERMOCHEMICAL NONEQUILIBRIUM SIMULATION APPROACH

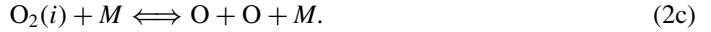
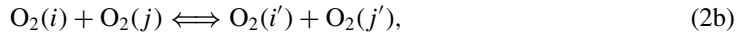
A. STS approach

The STS method tracks the temporal and spatial variation of molecules in each energy state by treating them as distinct species. Molecules at each energy state are portrayed by an individual continuity equation. Therefore, the governing equations of 1D inviscid and steady flow are

expressed as

$$\begin{aligned}\frac{\partial}{\partial x}(\rho_s u) &= \omega_s, \quad s = 1, 2, 3, \dots, n, \\ \frac{\partial}{\partial x}(\rho u^2 + p) &= 0, \\ \frac{\partial}{\partial x}\left[\rho u\left(h + \frac{1}{2}u^2\right)\right] &= 0,\end{aligned}\tag{1}$$

where x denotes the distance behind the shock; ρ denotes the density; s represents the species; u , p , and h denote the velocity, pressure, and enthalpy of the fluid, respectively; and ω is the change rate expressed in terms of density. For the O_2 binary mixture, which consists of O_2 and O , the reactions involved in the process are vibration-translation (V-T) (2a), vibration-vibration-translation (V-V-T) (2b), and dissociation-recombination (Dis-Rec) reactions (2c), which are shown as



In Eqs. (2) M represents the colliding particle, which could be O or O_2 . The indices i , j , i' , j' represent the states of O_2 . According to the STS method, the change rates of the numerical density of oxygen molecules induced by the transitions and chemical reactions are expressed as

$$\begin{aligned}\frac{d[\text{O}_2(i)]}{dt} &= k_{\text{Rec},m}^i[\text{O}_2][\text{O}]^2 - k_{\text{Dis},m}^i[\text{O}_2(i)][\text{O}_2] + k_{\text{Rec},a}^i[\text{O}]^3 - k_{\text{Dis},a}^i[\text{O}_2(i)][\text{O}] \\ &+ \sum_{j \neq i} \{k_{\text{V-T},m}^{j \rightarrow i}[\text{O}_2(j)][\text{O}_2] - k_{\text{V-T},m}^{i \rightarrow j}[\text{O}_2(i)][\text{O}_2]\} \\ &+ \sum_{j \neq i} \{k_{\text{V-T},a}^{j \rightarrow i}[\text{O}_2(j)][\text{O}] - k_{\text{V-T},a}^{i \rightarrow j}[\text{O}_2(i)][\text{O}]\} \\ &+ \sum_{i'} \sum_j \sum_{j'} \{k_{\text{V-V-T}}^{j,j' \rightarrow i,i'}[\text{O}_2(j)][\text{O}_2(j')]\} - \sum_{i'} \sum_j \sum_{j'} \{k_{\text{V-V-T}}^{i,i' \rightarrow j,j'}[\text{O}_2(i)][\text{O}_2(i')]\}, \tag{3}\end{aligned}$$

where k is the reaction rate coefficient; the subscripts V-T, V-V-T, Rec, and Dis represent specific processes, respectively; and m and a represent colliding particles as molecules or atoms. The superscript indicates the specific reaction; for example, $i \rightarrow j$ for the V-T reaction indicates the collision of $\text{O}_2(i)$ to form $\text{O}_2(j)$. $[\text{X}]$ indicates the number density of arbitrary particle X. Similarly, the number density change rate of O is obtained by considering only dissociation and recombination reactions, as shown by

$$\begin{aligned}\frac{d[\text{O}]}{dt} &= -2 \sum_i \{k_{\text{Rec},m}^i[\text{O}_2][\text{O}]^2 + k_{\text{Rec},a}^i[\text{O}]^3\} \\ &+ 2 \sum_i \{k_{\text{Dis},m}^i[\text{O}_2(i)][\text{O}_2] + k_{\text{Dis},a}^i[\text{O}_2(i)][\text{O}]\}.\end{aligned}\tag{4}$$

The relationship of the source term ω represented by density and the change rate of numerical density is given by

$$\omega_s = \frac{d[s]}{dt} \frac{M_s}{N_A}, \tag{5}$$

TABLE I. Reaction types and the sources of rates.

Reaction	Rate source
O ₂ Dis-Rec	Da Silva [50]
O ₂ -O V-T	Da Silva [50]
O ₂ -O ₂ V-T	FHO [51,52]
O ₂ -O ₂ V-V-T	FHO [51,52]
N ₂ Dis-Rec	Fangman [53]
N ₂ -N V-T	Fangman [53]
N ₂ -N ₂ V-T	Fangman [53]
N ₂ -N ₂ V-V-T	FHO [51,52]

where M_s is the molar mass of species s and N_A denotes Avogadro's number. Thermochemical nonequilibrium flow can be simulated using the STS method by combining these rates of change with the flow governing Eq. (1).

In this investigation, we consider all V-T process and mono-quantum V-V-T process. The sources of rates are detailed in Table I.

The STS approach constitutes a reliable benchmark for model evaluation, as it meticulously describes reaction processes with few assumptions. The program used in this paper to implement the STS approach for O₂ has been validated in a prior study [54]. Figure 1 illustrates the verification of postshock N₂ temperatures simulated in our study compared to the results obtained from the STS method and the direct molecular simulation (DMS) conducted by Fangman [53] and Schwartzentruber [55], respectively.

The results depicted in Fig. 1 demonstrate that present results are consistent with those of other researchers, indicating the accurate implementation of the STS method in the present study. Furthermore, the agreement between the STS [53] and DMS [55] results also validates the accuracy of the rate coefficients provided by Fangman. Additionally, in the model verification section of this article, the 1D simulation results are also verified against experimental data [56] and simulation results [53].

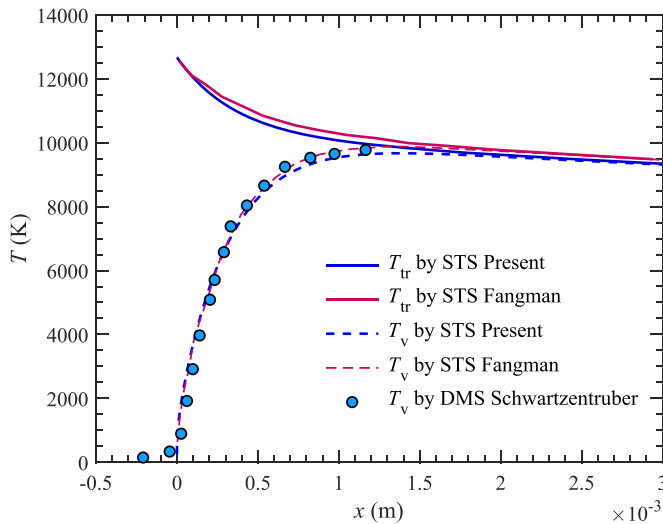


FIG. 1. Verification of STS simulation of N₂. Before the shock: Mach number $Ma_0 = 10.28$, temperature $T_0 = 295$ K, pressure $p_0 = 266.364$ Pa.

B. Two-temperature (2-T) model

1. Governing equations and dissociation rate coefficient

In addition to the STS method, this study employs the 2-T model for comparison. In the 2-T model, details regarding the number density of each vibrational energy level are blurred, treating vibrational energy as a whole. An additional vibrational energy equation has been incorporated to elucidate the translational-vibrational energy relaxation process. The governing equations are as follows:

$$\begin{aligned}
 \frac{\partial}{\partial x}(\rho_s u) &= \omega_s, \quad s = 1, 2, \\
 \frac{\partial}{\partial x}(\rho u^2 + p) &= 0, \\
 \frac{\partial}{\partial x} \left[\rho u \left(h + \frac{1}{2} u^2 \right) \right] &= 0, \\
 \frac{\partial}{\partial x} [\rho u e_v] &= \omega_{t-v} + \omega_{v-d},
 \end{aligned} \tag{6}$$

where the same symbols as in Eq. (1) indicate the same meaning; e_v represents specific vibrational energy; ω_{v-d} denotes the change of e_v induced by chemical reactions; ω_{t-v} represents the relaxation between translational and vibrational energy, which is calculated by the Landau-Teller (L-T) theory,

$$\omega_{t-v} = \frac{e_{v,\text{eq}}(T_{\text{tr}}) - e_v}{\tau}, \tag{7}$$

where $e_{v,\text{eq}}(T_{\text{tr}})$ is the equilibrium e_v at T_{tr} ; and τ is the characteristic relaxation time.

In this study, we derived the equilibrium chemical reaction rates for each 2-T model by weighting the reaction rates of individual energy states in the STS method according to the equilibrium distribution. Consequently, the equilibrium reaction rates at the same temperature are consistent across all models. This implies that any discrepancies observed between different models can be attributed solely to the approaches of nonequilibrium correction of each model.

The distinctions among various 2-T models primarily lie in their dissociation rate coefficients and the dissociation vibrational energy loss. For the Park model, the dissociation rate is calculated by

$$k_{\text{dis,Park}} = k_{\text{dis,eq}}(T_{\text{tr}}^a T_v^{1-a}). \tag{8}$$

The parameter a is recommended to be 0.5–0.7 [57], and we choose 0.5 in this study.

The rate expression of SGLME model was initially proposed by Colonna [38] and can also be derived from the maximum entropy criterion [39]. The dissociation rate of the SGLME model can also be expressed in terms of T_{tr} and T_v :

$$k_{\text{dis,SGLME}} = \sum_s k_{\text{Dis}}^s(T_{\text{tr}}) f_{\text{B}}(s, T_v). \tag{9}$$

In Eq. (9), s represents the specific energy state number, k_{Dis}^s signifies the dissociation rate coefficient of molecules in energy state s at T_{tr} , and $f_{\text{B}}(s, T_v)$ indicates the proportion of molecules in energy state s following the Boltzmann distribution at T_v . In summary, the dissociation rate of each state and state distribution of this model is determined by T_{tr} and T_v , respectively, and the total dissociation rate of molecules is obtained by weighting the dissociation rates of individual energy states according to the distribution of energy states. Thus, this model comprehensively captures the

TABLE II. The discrepancy between τ with τ_{ave} and τ_{fit} during isothermal isobaric relaxation of N_2 and O_2 that T_v is 270.6 K initially.

	$T_{\text{tr}}(\text{K})$	$\tau_{\text{ave}}(\text{s})$	$(\tau_{\text{ave}} - \tau /\tau_{\text{ave}})_{\text{max}}$	$(\tau_{\text{ave}} - \tau /\tau_{\text{ave}})_{\text{ave}}$	$(\tau_{\text{fit}} - \tau /\tau_{\text{fit}})_{\text{max}}$	$(\tau_{\text{fit}} - \tau /\tau_{\text{fit}})_{\text{ave}}$
O_2	3000	1.4869^{-6}	10.01%	2.64%	15.56%	12.52%
	5000	2.8275^{-7}	27.94%	8.15%	24.27%	17.21%
N_2	5000	7.6587^{-6}	30.81%	7.96%	26.62%	5.55%
	8000	1.2247^{-6}	15.82%	5.30%	14.23%	7.77%

impact of nonequilibrium of different internal energy modes while disregarding the influence of NB effects.

2. Verification of calculation of internal energy relaxation

The L-T theory is widely used to describe the internal energy relaxation process in 2-T models. The L-T theory posits that the characteristic relaxation time, τ , depends only on the component and T_{tr} . While the theory assumes molecules are harmonic oscillators, diatomic molecules are anharmonic oscillators. Consequently, τ is influenced by factors like energy state distribution changes during the process. Thus, we use the STS method to simulate τ fluctuations for anharmonic oscillator molecules. If τ does not change significantly, the L-T theory can still accurately describe the internal energy relaxation process for these molecules.

For simulations, the initial T_v is set at 270.6 K. Isothermal isobaric relaxation processes are performed with a constant T_{tr} . The relaxation characteristic time τ , vibrational energy e_v , and equilibrium vibrational energy $e_{v,\text{eq}}(T_{\text{tr}})$ are calculated and shown in Fig. 2. The fitted τ values by Hao [58] and Fangman [53] for O_2 and N_2 , respectively, are also displayed. The τ computed by the STS method is derived using Eq. (7) and the STS simulation results. Hao provides fitting equations for τ of the collision pairs $\text{O}_2\text{-O}$ and $\text{O}_2\text{-O}_2$. Fangman provides τ for $\text{N}_2\text{-N}_2$ and $\text{N}_2\text{-N}$ at various temperatures, and we used interpolation to determine τ at other temperatures. The τ of the mixed system components is calculated by weighting the τ of each collision pair by number density. Equilibrium time t_0 is defined as the first time when $e_{v,\text{eq}} - e_v \leq 0.02e_{v,\text{eq}}$. The horizontal coordinate \bar{t} is then made dimensionless by t_0 .

From the outcomes in Fig. 2, it is evident that the variation in τ during the internal energy relaxation process is negligible until the system approaches equilibrium. Table II presents τ_{ave} , the average value of τ , along with the average and maximum percentage deviations of τ from τ_{ave} and τ_{fit} obtained by the fitting equations from Hao and Fangman. According to Table II, except for the τ_{fit} of O_2 , the mean deviation between τ and both τ_{ave} and τ_{fit} is less than 9%. Figure 2(a) shows that the difference between τ obtained by the STS method and τ_{fit} of O_2 is negligible at the beginning of the process, when vibrational energy is far from equilibrium and internal energy relaxation is intense. The deviation mainly occurs near equilibrium, where its effect on relaxation is minimal. Furthermore, internal energy relaxation is much faster than chemical reactions in these cases, with molecule-molecule collisions dominating the relaxation process and determining τ . The variation of τ for molecule-molecule collisions is small at constant T_{tr} . Thus, the L-T theory reasonably approximates τ as a constant. The specific values of τ_{fit} provided by Hao [58] and Fangman [53] closely match the STS results. Therefore, the error introduced by using the L-T theory to describe the relaxation process is acceptable.

In the original maximum entropy model, the internal energy relaxation process is determined by calculating the actual molecule involvement in transitions after the reconstructed distribution [39]. In this study, we propose an improved model that introduces a correction factor based on the SGLME model, meaning the reconstructed distribution by the SGLME model cannot reflect the actual state distribution. Consequently, using the previous methodology to calculate the relaxation process would be erroneous and misleading. To address this issue, we also utilize the L-T theory,

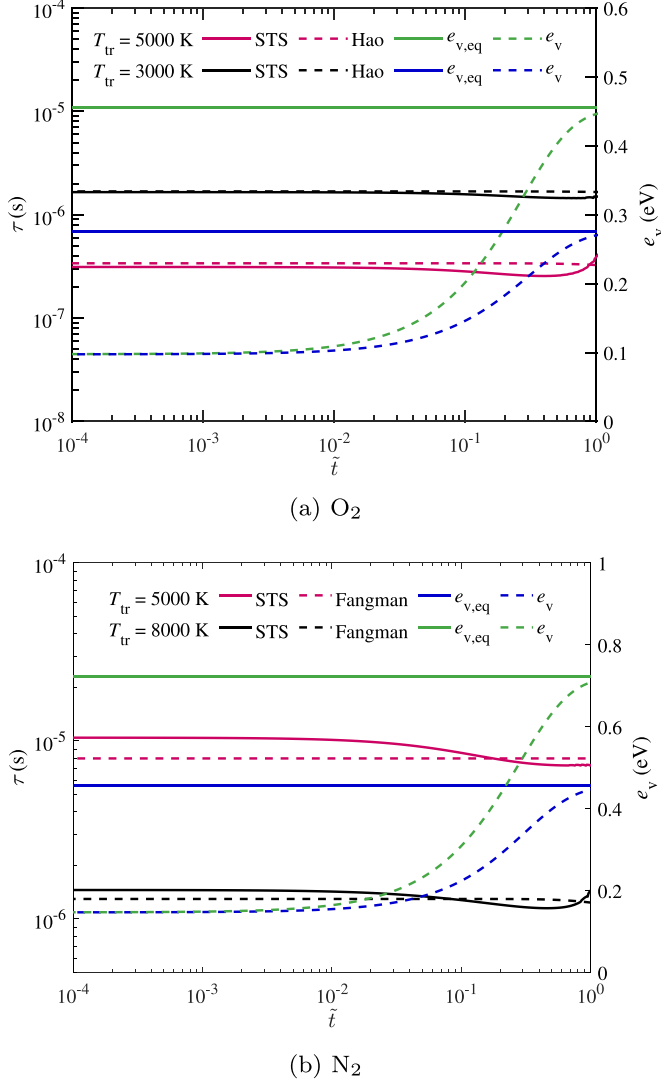


FIG. 2. The characteristic relaxation time τ , vibrational energy e_v , and equilibrium vibrational energy $e_{v,eq}$ during the isothermal-isobaric relaxation process, with initial $T_v = 270.6$ K and different T_{tr} for O₂ and N₂, are obtained using the STS method. The fitted τ_{fit} by Hao [58] and Fangman [53] are also shown.

along with the τ by Hao [58] and Fangman [53], to characterize the internal energy relaxation process in the improved model introduced later.

3. Verification of calculation of vibrational energy loss during dissociation

Next, we verified the assumption regarding the vibrational energy change rate induced by chemical reactions, ω_{v-d} , through the STS method. Initially, T is set at 270.6 K, then T_{tr} is suddenly increased to T_1 , followed by relaxation to equilibrium under isothermal-isobaric conditions. Figures 3 and 4 depict the ω_{v-d} per unit volume, as simulated by the STS method throughout the relaxation process. For comparison, the ω_{v-d} obtained by assuming the vibrational energy loss per net dissociation $e_{v,loss,s}$ is the average vibrational energy e_{ave} , 0.5, and 0.7 times the dissociation energy (D_0) are also shown. This method intuitively shows which stage of dissociation is more intense,

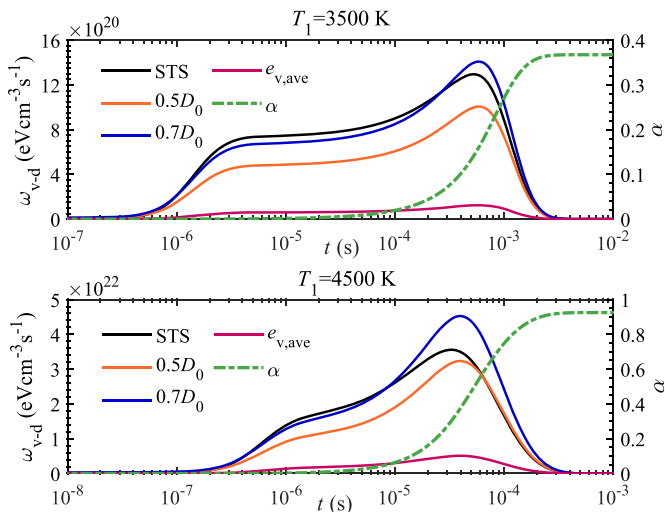


FIG. 3. The isothermal-isobaric relaxation process of O_2 simulated by the STS method with an initial temperature T_0 of 270.6 K and various translational temperatures T_1 . The ω_{v-d} due to chemical reactions per unit volume simulated by STS, as well as the results obtained by assuming the vibrational energy loss per dissociation $e_{v,loss,s}$ to be $e_{v,ave}$, $0.5D_0$, and $0.7D_0$ are shown, respectively. The variation of α during the relaxation process is also shown.

helping to avoid anomalies caused by numerical calculations when the net dissociation amount is minimal near equilibrium. The dissociation degree α is also illustrated in these figures, defined by

$$\alpha = \frac{[X]}{[X] + 2[X_2]} \quad (10)$$

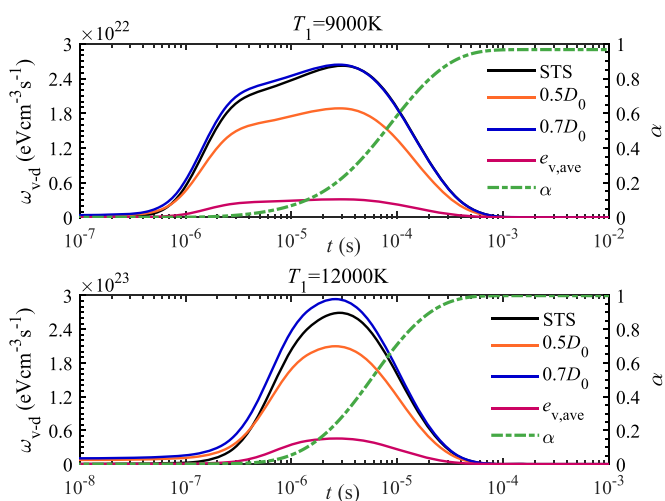


FIG. 4. The isothermal-isobaric relaxation process of N_2 was simulated using the STS method with an initial temperature T_0 of 270.6 K and various translational temperatures T_1 . The ω_{v-d} according to different assumptions and α are shown. The meaning of the curves and legends is the same as in Fig. 3.

As the figures show, $e_{v,\text{loss},s}$ falls within the range of 0.5–0.7 times D_0 . Hong [32] analyzed the O_2 stagnation streamline flow and found that energy loss is also approximately 0.3–0.5 times the dissociation energy. These results indicate that the assumption in the Park model, which considers the vibrational energy loss due to dissociation during the relaxation process to be $0.5D_0$, is reasonable.

Figure 4 indicates that the pattern of dissociation vibrational energy loss for N_2 in the STS simulation is similar to that of O_2 , with values also ranging between approximately 0.5 and $0.7D_0$. Furthermore, Wang [59] concluded that the value of energy loss per dissociation has minimal influence on the process. Their calculations show that changing the $e_{v,\text{loss},s}$ by $0.5D_0$ has limited impact on the final results. The results of this study show that the $e_{v,\text{loss},s}$ during the above process compared to the commonly used assumption value of $0.5D_0$ in the Park model is at most about $0.2D_0$. Consequently, this assumption is not expected to significantly impact the results. Thus, we adopted $0.5D_0$ as the value of $e_{v,\text{loss},s}$ for the Park model in our study.

For the SGLME model, the expression for vibrational energy loss in dissociation is

$$\begin{aligned} e_f &= \frac{\sum_s \{k_{\text{Dis}}^s(T_{\text{tr}})f_{\text{B}}(s, T_v)e_s\}}{\sum_s \{k_{\text{Dis}}^s(T_{\text{tr}})f_{\text{B}}(s, T_v)\}}, \\ e_b &= \frac{\sum_s \{k_{\text{Rec}}^s(T_{\text{tr}})e_s\}}{\sum_s \{k_{\text{Rec}}^s(T_{\text{tr}})\}}, \\ e_{v,\text{loss},s} &= \frac{\omega_b e_b - \omega_f e_f}{\omega_b - \omega_f}, \end{aligned} \quad (11)$$

where e_s is the vibrational energy of molecules at state s , and f and b represent the forward and backward reactions, respectively.

For the same reasons as internal energy relaxation, dissociation rate coefficients in the improved model are not solely dependent on number density. This makes determining the energy level distribution of molecules involved in dissociation impossible. To address this, we adopt a similar approach to the Park model and assume $e_{v,\text{loss},s}$ upon dissociation is $0.5D_0$.

In this section, we introduced the simulation methods used in this study and verified certain assumptions and parameter selections in the traditional 2-T model. We confirmed that errors introduced by the calculation methods for the internal energy relaxation source term and the dissociation vibrational energy loss term in the conventional 2-T model are negligible. Consequently, discrepancies between the simulation results of the 2-T model and experimental results primarily arise from inaccurate calculations of dissociation rate coefficients, with the uncorrected NB effect being a significant factor. Therefore, the next section focuses on NB correction of the dissociation rate coefficient in the improved model.

III. THE IMPROVED MODEL

A. The influence of NB effect on dissociation rate

The impact of thermal nonequilibrium on the dissociation rate can be theoretically categorized into two aspects: nonequilibrium between different internal energy modes and the NB effect [45,54,55]. In this article, the term “internal energy nonequilibrium” specifically refers to the former. The SGLME model effectively captures the influence of internal energy nonequilibrium on the dissociation rate. Thus, we selected dissociation rates calculated using the STS method and the SGLME model to define the influence factor of the NB effect, denoted as ζ [54]. The expression for ζ is

$$\zeta = \frac{k_{\text{Dis,STS}}}{k_{\text{Dis,SGLME}}}. \quad (12)$$

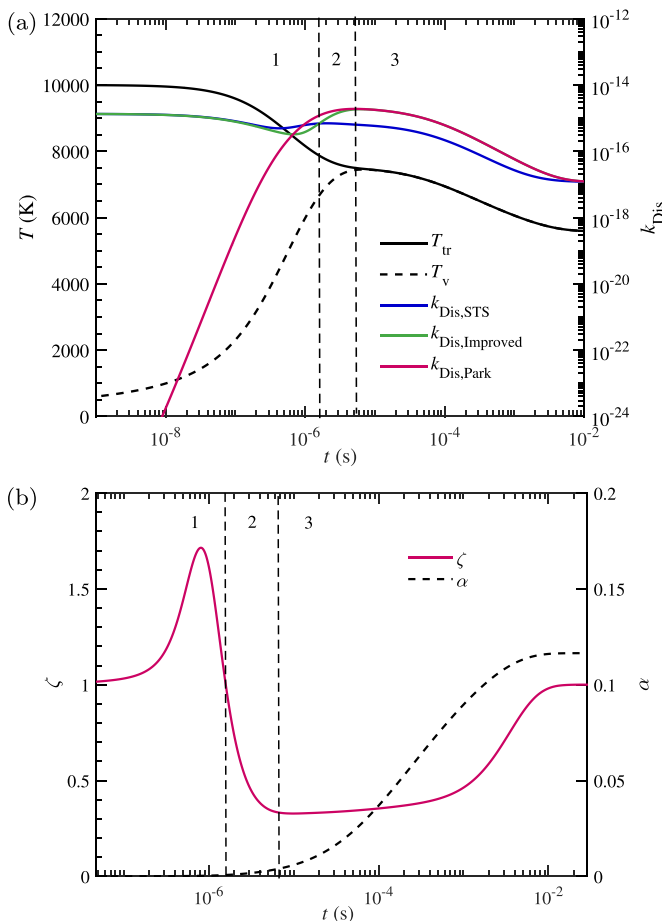


FIG. 5. 0D N_2 adiabatic relaxation process, with $T_0 = 270.6$ K, $p_0 = 0.1$ atm initially. Then the T_{tr} surges to 10 000 K and the system relaxes to equilibrium. (a) Temperature and dissociation rates calculated by different models; (b) NB factor ζ and degree of dissociation α .

We develop an improved model that integrates the SGLME model and ζ to capture the influence of thermochemical nonequilibrium on dissociation. Initially, we examined the NB effect using ζ . A previous study had delved into the NB effect of O_2 [54]. In the heating relaxation process of O_2 , it was observed that the dissociation rate coefficients initially exceeded the equilibrium dissociation rate due to the NB effect. As the internal energy reached equilibrium, the dissociation rate significantly decreased until the system was fully equilibrated. This study aims to explore whether the NB effect of N_2 during the heating nonequilibrium process exhibits a similar trend.

To this end, we performed simulations using the STS method, initializing the system at $p_0 = 0.1$ atm and 295 K in equilibrium. A rapid increase in T_{tr} to 10 000 K was then applied, followed by relaxation to equilibrium under adiabatic conditions. Figure 5 illustrates the temperature, ζ , and dissociation degree, α . Additionally, dissociation rate coefficients calculated by different models based on T_{tr} , T_v , and energy state distribution are shown.

Based on the curves in Fig. 5, it is evident that the dissociation rate of N_2 exceeded the equilibrium dissociation rate in the early stage of the process, reflected by an increase in ζ . This phenomenon occurs because the high T_{tr} initially causes the distribution of molecules to transition to high energy levels far beyond the equilibrium distribution corresponding to T_v , thereby accelerating

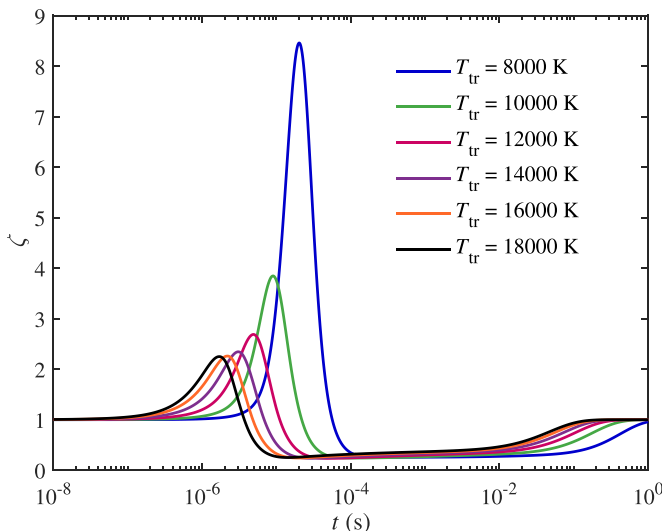


FIG. 6. The variation of ζ for N_2 in adiabatic relaxation with an initial T_v of 295 K and different initial T_{tr} .

the overall dissociation rate. This distribution results from multiquantum V-T transitions occurring in molecule-molecule collisions, as energy levels follow a Boltzmann distribution when such processes are neglected [28]. As T_v increases, it becomes increasingly difficult for transitions to replenish the high-energy level particles involved in dissociation to the equilibrium distribution corresponding to T_v . Consequently, ζ gradually decreases to its minimum value, indicating that the NB effect leads to a lower dissociation rate.

As the relaxation process continues, the rate of dissociation reactions decreases, with transitions gradually leading the energy level distribution toward equilibrium. This is manifested by a gradual increase in ζ . Ultimately, the system reaches equilibrium, and ζ returns to 1, indicating that the vibrational level distribution is also in equilibrium. Based on the analyzed characteristics of ζ , we categorize the variation of the NB effect during the relaxation process into three stages: (1) $\zeta > 1$, (2) ζ decreasing from 1 to the minimum value ζ_{\min} , and (3) ζ recovering from ζ_{\min} to 1. This stage division is illustrated in Fig. 5, and the reproduction of the NB effect correction factor ζ in Sec. III B is also based on this division.

Figure 6 displays the variation of the NB effect under different initial T_{tr} . Specific numerical comparisons show that in the early relaxation phase, where the rate exceeds the equilibrium distribution rate due to overdistribution of high-state molecules, lower temperature conditions exhibit a larger ζ . This occurs because these conditions have lower T_v , resulting in a smaller baseline $k_{Dis, SGLME}$. A similar trend is observed in Singh's research [42]. Subsequently, in the stage where dissociation leads to an underdistribution of high-state molecules, the minimum value of ζ is slightly higher at higher temperatures. Overall, the variation of ζ during the relaxation process at different temperatures follows the pattern of an initial increase in dissociation rate due to the overdistribution of high-state molecules, followed by a decrease due to the consumption of these molecules.

Comparing the NB effect on O_2 [54] and N_2 during the heating thermochemical nonequilibrium relaxation process, we found that their influence on dissociation rate exhibits similar trends and differs only in specific values. Therefore, the NB effect of different types of collision pairs can be portrayed in a unified form.

Next, it's necessary discuss the validity of applying the empirical formula derived from the 0D nonequilibrium relaxation process to correct the NB effect in various scenarios. Previous research [54] indicates that during the heating nonequilibrium process of diatomic molecules, the sum of the stoichiometric number of dissociation and transition, which are dominant, is equalized.

Therefore, pressure only influences the NB effect when the system is near equilibrium, where the recombination reaction is significant. Under these conditions, temperature becomes the main factor affecting the relative relationship of physical quantities in nonequilibrium processes. Considering that temperature cannot reflect the change in the zero-point energy of the particles due to component changes caused by chemical reactions, we choose the equilibrium dissociation degree α_{eq} as another parameter for portraying the relaxation process, providing a comprehensive description of the system's current energy. A previous study [54] also indicates that the influence of the NB effect remains consistent between 0D chemical reactions with similar temperature variations and processes involving flow. The NB effect in flow aligns more closely with slightly higher temperature cases in 0D relaxation processes due to the conversion of kinetic and internal energy. α_{eq} also reflects the influence of this energy conversion. Thus, the influence of the NB effect during thermochemical nonequilibrium flow relaxation is similar to that during 0D adiabatic relaxation. In conclusion, it is reasonable to derive fitting equations for the correction factors ζ based on 0D nonequilibrium processes and extend their application to other processes with similar temperature variations.

B. Fitted formula of NB effect correction factor

Based on the preceding analysis, this study uses dissociation rate coefficients calculated with the SGLME model and integrates them with the NB effect correction factor to establish an improved model. Chemical reactions are significantly influenced by the NB effect and are a major contributor to its occurrence. The relationship between the NB effect and the progression of chemical reactions during relaxation remains largely consistent across different flow conditions [28,54]. Consequently, we use the chemical reaction progress δ ,

$$\delta = \frac{\alpha}{\alpha_{\text{eq}}}, \quad (13)$$

to formulate a fitting formula for ζ representing the NB effect, enhancing the accuracy of the dissociation rate coefficient. By incorporating a correction factor for the NB effects into the rate coefficients calculated using the SGLME model, we present a comprehensive description of the dissociation rate coefficients under thermochemical nonequilibrium conditions, as expressed by

$$k_{\text{Dis}} = \zeta k_{\text{Dis, SGLME}}. \quad (14)$$

Next, we introduce the specific construction of the fitting formula for ζ . For any relaxation process, α_{eq} represents the equilibrium dissociation degree at the current state. Based on this, δ signifies the direction of chemical nonequilibrium: $\delta < 1$ corresponds to dissociation-dominated processes, while $\delta > 1$ refers to recombination-dominated processes. This paper focuses on dissociation resulting from a sudden temperature increase, where $\delta < 1$.

As discussed in Sec. III A, during the nonequilibrium process induced by heating, the NB effect factor ζ on the dissociation rate initially increases, then decreases to a minimum value, and finally returns to 1 as the system approaches equilibrium. To accurately depict this behavior, we describe the NB effect in segments based on its distinct trends.

In the early stages of the relaxation process, when the system is far from equilibrium, the chemical reaction is vigorous and occurs on a short timescale. At this stage, ζ_{av} , the average value of ζ provides a meaningful representation of the NB effect on the dissociation rate coefficients. To balance the accuracy of the correction with the complexity of the fitting equation, we choose the ζ_{av} to describe the influence of the NB effect during this stage as

$$\zeta_1 = \zeta_{\text{av}}. \quad (15)$$

During this stage, higher total energy corresponds to higher T_v , resulting in higher dissociation rate coefficients calculated by the SGLME model [54]. Since the SGLME model serves as the baseline for assessing the NB effect, a higher equilibrium dissociation degree α_{eq} leads to larger rate coefficients, resulting in a smaller ζ_{av} . Thus, ζ_{av} for different species is negatively correlated with

TABLE III. Parameters in fitted formula.

	b_1	b_2	ζ_{av}	ζ_{min}	δ_1	k_l
O ₂ -O	27	11	$-2.17\alpha_{eq} + 2.2546$	$0.31\alpha_{eq} + 0.27$	$0.3433\alpha_{eq} - 0.005$	$0.15\alpha_{eq} + 0.01$
O ₂ -O ₂	27	11	$-2.17\alpha_{eq} + 2.2546$	$0.31\alpha_{eq} + 0.27$	$0.3433\alpha_{eq} - 0.005$	$0.15\alpha_{eq} + 0.01$
N ₂ -N	37.5	5.2	$-0.31\alpha_{eq} + 1.35$	$0.155\alpha_{eq} + 0.35$	$0.3433\alpha_{eq}$	$0.03\alpha_{eq} + 0.02$
N ₂ -N ₂	37.5	5.2	$-0.89\alpha_{eq} + 1.49$	$0.40\alpha_{eq} + 0.216$	$0.3433\alpha_{eq}$	$0.03\alpha_{eq} + 0.02$

α_{eq} . The value δ_1 , indicating the δ at the end of the first stage, is controlled by α_{eq} and determines the boundary between the first and second stages.

In the subsequent stage, we focus on the reduction of ζ from ζ_{av} to the minimum value (ζ_{min}). The expression for this decrease is given by

$$\zeta_2 = \zeta_{min} + (\zeta_{av} - \zeta_{min})\exp\left(\frac{\delta_1 - \delta}{k_l}\right), \quad (16)$$

which facilitates a rapid decrease in ζ as dissociation progresses. For the processes studied, the specific internal energy of the system is reflected in α_{eq} , significantly influencing the rates of transitions and chemical reactions for N₂ and O₂. These processes determine the number density distribution of high-energy level molecules, impacting the NB effect. Therefore, the parameter k_l , controlling the rate of ζ decrease, is also determined by α_{eq} .

In the later stage, the total internal energy across different modes approaches equilibrium, making the NB effect the dominant nonequilibrium influence. During this phase, ζ gradually recovers from ζ_{min} to 1. The NB effect in this stage is primarily influenced by chemical reactions, and we continue to describe ζ according to the chemical reaction progress δ .

As T_{tr} increases, α_{eq} become higher and chemical reactions become more vigorous, prolonging the duration of the NB effect. Consequently, the variation of ζ , representing the NB effect, is correlated with α_{eq} . To control the recovery rate of ζ , we choose $b_1\alpha_{eq} + b_2$. This results in a slower recovery of ζ to 1 in systems with higher α_{eq} , indicating that the NB distribution takes longer to fully recover and reach equilibrium distribution. The final expression obtained is given by

$$\zeta_3 = (1 - \zeta_{min})\frac{\exp(\delta * (b_1\alpha_{eq} + b_2)) - 1}{\exp(b_1\alpha_{eq} + b_2) - 1} + \zeta_{min}. \quad (17)$$

This formulation ensures that when the dissociation progress δ reaches 1, ζ also reaches 1, signifying that the dissociation rate returns to equilibrium rate. Thus, Eq. (17) ensures that no NB effect persists when the system reaches equilibrium.

The corrections described above apply specifically to dissociation-dominated processes. The continuity between the first and second stages is governed by Eq. (16). To ensure a smooth transition, Eqs. (16) and (17) are made continuous by selecting the maximum value between them. The final form of ζ is the following:

$$\begin{aligned} \delta > 1: & \quad k_{Dis} = k_{SGLME} \\ \delta < 1: & \quad k_{Dis} = \zeta k_{SGLME} \\ \zeta = & \begin{cases} \zeta_{av}, & \delta < \delta_1 \\ \max(\zeta_2, \zeta_3), & \text{else} \end{cases}. \end{aligned} \quad (18)$$

Combining ζ with the SGLME model as shown in Eq. (14), we establish a framework for dissociation rate coefficients in the improved model. Specific parameter values for different collision pairs of various stages are summarized in Table III.

Figure 7 presents a detailed comparison between ζ obtained from the fitting formula for the O₂-O process and those computed in the actual simulation at initial $T_{v0} = 295$ K and various initial translational-rotational temperatures T_{tr0} .

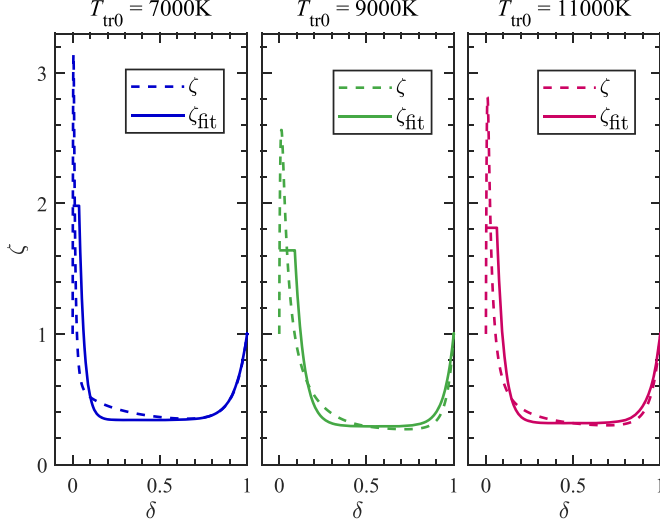


FIG. 7. The comparison of fitted formula ζ_{fit} and actual value of ζ of several T_{tr0} .

The average correction factor ζ_{av} in the first stage accurately represents the relative magnitude of the NB effect's influence at different temperatures. In subsequent stages, ζ effectively reflects the NB effect on the dissociation rate, considering the progression of δ and the influence of α_{eq} .

The above analysis is based on 0D relaxation processes. The literature [28,54] suggests that recreating and analyzing flow thermochemical conditions based on 0D simulations is both theoretically and quantitatively feasible. Therefore, the correction factor ζ remains applicable in practical flows, requiring only the calculation of α_{eq} based on local temperature, pressure, and composition of the flow.

In the next section we will validate the correction effect of ζ in flow after a normal shock.

IV. VERIFICATION OF IMPROVED MODEL

In this section, we will simulate the nonequilibrium process following a normal shock for N_2 and O_2 separately. The postshock parameters will be obtained based on the Rankine-Hugoniot (R-H) relationship. The computational results of the improved model will be compared and verified against those of the STS method, the SGLME model, and the Park model, aiming to analyze the correction effects and identify any deficiencies.

A. Verification of results for O_2

In this subsection, we validate the NB effect in O_2 relaxation processes after a normal shock using the improved model, comparing it with experimental data and STS method results. Experimental dissociation degree data is available only for Case 3. T_v is defined by the number density of molecules in the ground and first excited energy states as

$$T_v = \frac{e_v(1) - e_v(0)}{-k_b \ln\{[O_2(1)]/[O_2(0)]\}}, \quad (19)$$

where k_b is the Boltzmann constant.

The parameters before the shock for the O_2 cases are presented in Table IV, including the Mach number (Ma_0), pressure (p_0), and temperature (T_0).

The calculated results of the postshock relaxation process of O_2 for Case 1 are illustrated in Fig. 8. With a postshock temperature is approximately 5000 K, dissociation is relatively weak and

TABLE IV. Cases of verification for O_2 .

Case	Ma_0	p_0 (Pa)	T_0 (K)
1	9.37	266.364	295
2	12.62	133.182	295
3	13.55	106.546	295

the internal energy relaxation process predominates. Consequently, the Case 1 serves as a significant indicator of the computational effects of the L-T theory on internal energy relaxation. As discussed earlier in Sec. II B 2, The L-T theory, particularly with the τ fitting formula proposed by Hao [58], accurately characterizes internal energy relaxation for O_2 in our simulation. The results in Fig. 8 show good agreement between the internal energy relaxation processes predicted by the three 2-T models using the L-T theory and those from the STS approach. This underscores the accuracy of Hao's τ fitting formula and confirms the validity of the L-T theory for describing these relaxation processes.

Figure 9 illustrates the calculated results for Case 2. Initially, all models exhibit nearly identical results during the early stages of internal energy relaxation. However, as dissociation reactions become more pronounced in the later stages, the improved model calculations more closely align to those of the STS method than the SGLME model and the Park model.

As the internal energy relaxation process nears completion, T_{tr} and T_v approach similar values. The SGLME and Park models determine thermal equilibrium based on the difference of T_{tr} and T_v . Therefore, in flow where the internal energy relaxation is essentially completed, the system is considered to be in thermal equilibrium by these conventional 2-T models. Thus, in flow scenarios where internal energy relaxation is largely complete, these models disregard NB effects, resulting in consistent predictions. In subsequent cases, these two models also exhibit similar characteristics. Results from the STS method reveal a significant disparity between the dissociation rates obtained and the rates predicted by the 2-T models. This discrepancy can be attributed to the influence of the NB effect, which is not accounted for in the 2-T models but is critical in accurately predicting dissociation rates in such scenarios.

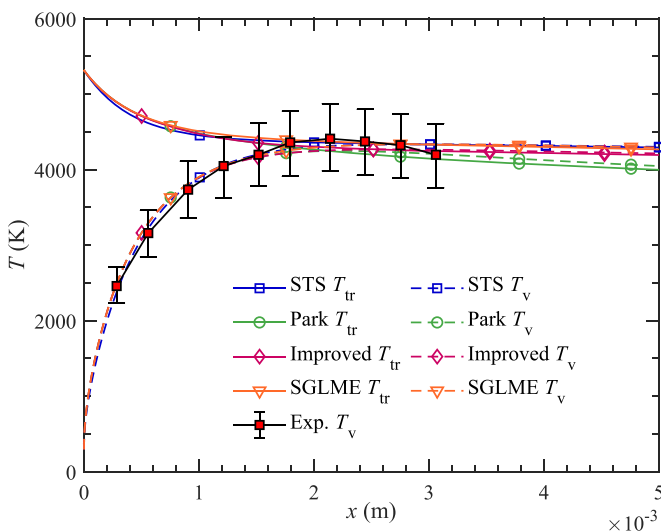


FIG. 8. Results of Case 1.

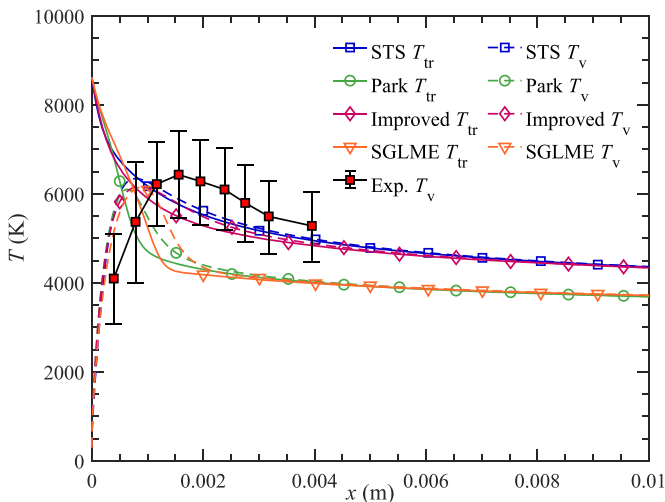


FIG. 9. Results of Case 2.

The improved model effectively captures the phenomenon of the NB effect reducing the dissociation rate of O_2 , aligning closely with results from the STS method. As the internal energy relaxation process approaches completion (near $x = 0.002$ m), the predicted T_{tr} by the improved model is slightly lower than that obtained from the STS method. This discrepancy primarily arises from the transition between ζ_2 and ζ_3 in the improved model, where the maximum value between the two is selected. Table VI summarizes the deviations of various model calculations from the STS method for each case. The maximum deviations of T_{tr} calculated by the improved model are within 6%, indicating minor and acceptable deviations in the simulations.

The temperature simulation for Case 3 is depicted in Figs. 10(a) and 10(b), while the dissociation degree is illustrated in Fig. 10(c). Due to T_{tr} and T_v being plotted in two separate plots, to facilitate comparison, dashed lines are added to indicate the region where the internal energy relaxation of each model is essentially completed in both temperature plots. To avoid misunderstanding, it's essential to clarify that although the results for this condition depict a relaxation process over a considerable distance following the shock, the system has not yet reached equilibrium in the displayed process. Therefore, the discrepancy at $x = 0.01$ m does not imply differences in equilibrium positions for each method. In this case, the dissociation degree α calculated by the STS method initially exhibits a noticeable deviation from the experimental data at the beginning of the process. As the relaxation process progresses, the difference between the calculated and experimental values gradually diminishes. The calculated temperatures and dissociation degree α show improved agreement with the experimental results, indicating that the STS method accurately simulates the thermochemical nonequilibrium process.

Comparing the results obtained from different models, it is observed that the Park model predicts a slightly lower degree of dissociation at the initial stages of the process, leading to a higher value of T_{tr} . This discrepancy arises because the Park model overlooks the presence of high-energy level molecules capable of rapid dissociation when T_v is low. Additionally, when internal energy relaxation is essentially complete, the Park and SGLME models neglect the NB effect, resulting in a significantly higher α in calculations compared to the other models. Calculations conducted with the improved model show minor deviations from the STS method, particularly at the aforementioned transition stage. However, the improved model yields consistent results with the STS method overall.

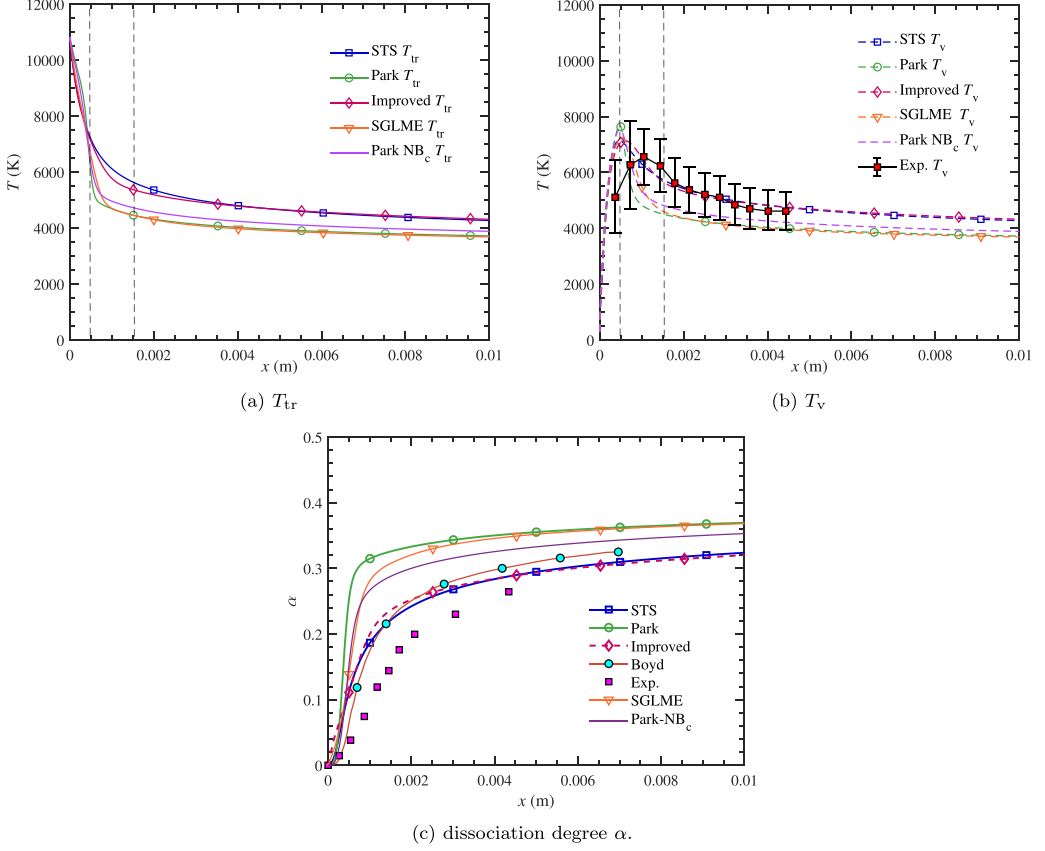


FIG. 10. Results of Case 3, Park-NB_C represents the result of Park model with NB correction proposed by Chaudhry.

In this case, we also verified the effectiveness of the correction factor proposed by Chaudhry [47] for the NB effect, as given by

$$\zeta_{NB,C} = \min \left\{ \exp \left[\ln(0.5) \left(1 - \frac{[X]^2}{k_{eq}[X_2]} \right) \right], 1 \right\}, \quad (20)$$

where k_{eq} is the dissociation equilibrium constant. According to its expression, this factor also reflects the phenomenon that, most of the time, NB effects lead to a decrease in the dissociation rate during the dissociation-dominated relaxation process. This factor can be integrated with any 2-T model to further correct the NB effect. Traditional 2-T models assume thermal equilibrium once internal energy relaxation is complete, leading to consistent dissociation rate coefficients. Incorporating this modified factor into the Park model allows us to simulate the equilibrium relaxation process following a normal shock and evaluate its impact. As shown in Fig. 10, compared to the original Park model results, temperatures and dissociation rates calculated using Chaudhry's correction factor more closely align with those calculated by STS. This indicates that Chaudhry's correction factor partially corrects the decrease in dissociation rate caused by the NB effect, although complete correction remains elusive.

Synthesizing the results of the three mentioned cases, in the thermochemical nonequilibrium relaxation process of O_2 in the postshock region, the L-T theory accurately describes internal energy relaxation process. Consequently, variations among different models primarily arise from

TABLE V. Cases of verification for N_2 .

Case	Ma_0	p_0 (Pa)	T_0 (K)
4	15.96	276.80	251.05
5	20.00	276.80	251.05
6	17.56	133.182	300.0

differences in the dissociation rate. The NB effect notably enhances the dissociation rate coefficient in the early stages compared to the equilibrium dissociation rate, leading to a more rapid decrease in T_{tr} for the models considering the NB effect. The change in T_{tr} during this stage is primarily driven by the component change due to the dissociation reaction, which involves energy conversion between translational-rotational energy and zero-point energy. Thus, the T_v calculated by different models shows minimal divergence. In the later stages of the relaxation process, results across all cases exhibit similar characteristics. Due to the neglect of the NB effect after the completion of internal energy relaxation, the traditional 2-T models and the SGLME model overestimate the dissociation rate, leading to an underestimation of T_{tr} . In contrast, the improved model effectively simulates the NB effect's influence on dissociation rates, yielding results consistent with those from the STS method.

B. Verification of results for N_2

Next, we will verify the improved model in the relaxation process of N_2 after a normal shock. The parameters before the shock for are presented in Table V. In this subsection, to facilitate comparison with the results of Fangman [53], T_v is defined by the specific vibrational energy e_v .

Figure 11 presents the results for Case 4 of the N_2 . In these cases, τ is determined through interpolation using the current T_{tr} and the corresponding τ value at partial T_{tr} provided by Fangman [53]. The calculated τ aligns well with the internal energy relaxation process based on the current STS data. Consequently, the results of internal energy relaxation across different models are consistent.

The results after the completion of internal energy relaxation from Case 4 will be jointly analyzed with those from Case 5, which are depicted in Fig. 12. Upon completing internal energy

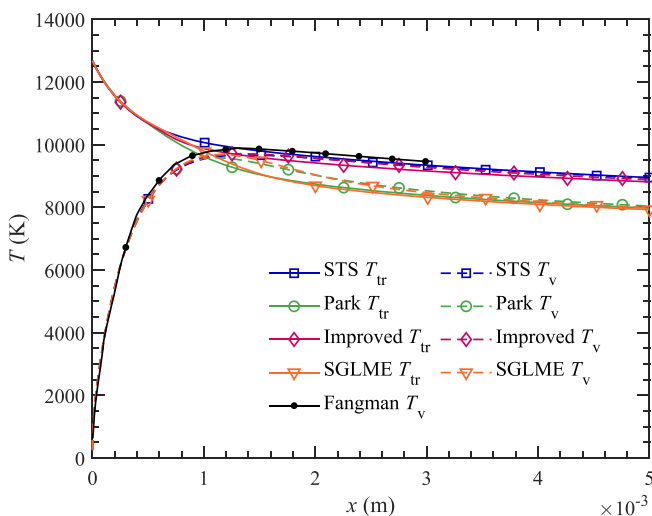


FIG. 11. Results of Case 4.

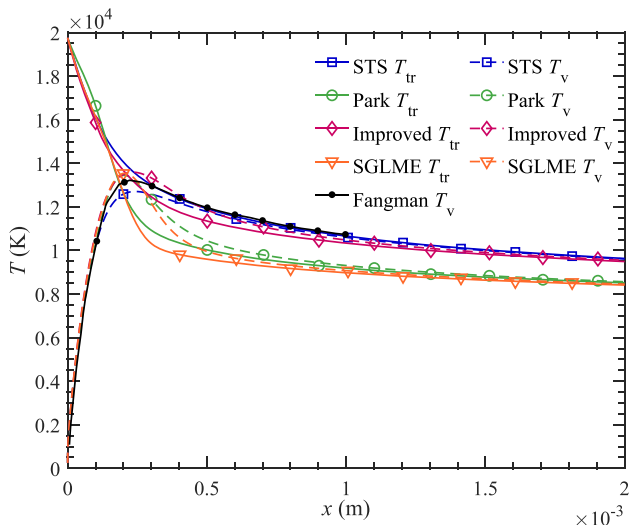


FIG. 12. Results of Case 5.

relaxation, the outcomes from Cases 4 and 5 suggest that the relaxation process of N_2 shares similar characteristics with that of O_2 in Sec. IV A. Obviously, the temperatures calculated by the STS method and the improved model, which account for the NB effect, are higher compared to those calculated by the Park model and the SGLME model. This temperature difference arises because the models considering the NB effect calculate a lower dissociation rate. Consequently, the dissociation reaction absorbs less energy, resulting in a higher temperature.

Figure 13 illustrates the results obtained from Case 6, where the computations extend over a significant distance in the postshock region to clearly observe the NB effect's impact. The results show that the temperatures calculated by the Park model and the SGLME model are notably lower than those calculated by the other two models for an extended distance after the shock. This disparity is due to the NB effect, which reduces the dissociation rate, resulting in higher temperatures. These

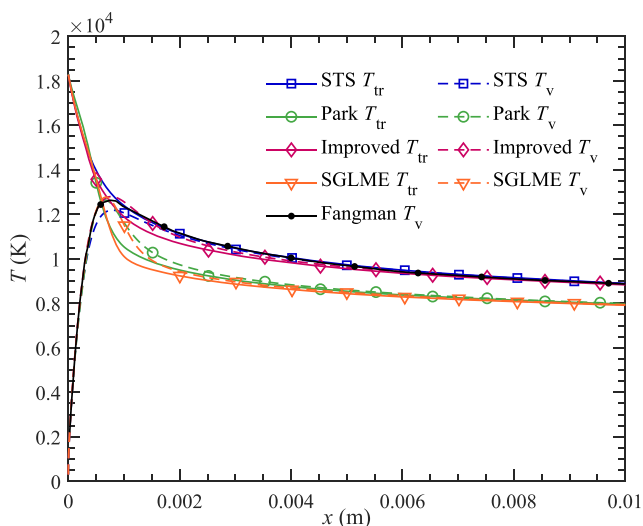


FIG. 13. Results of Case 6.

TABLE VI. The maximum and average discrepancy between temperatures by the STS method with the Park and improved models in Cases 1–6.

	Variant	Park _{max}	Improved _{max}	Park _{ave}	Improved _{ave}
Case 1	T_{tr}	9.91%	2.47%	5.98%	1.98%
	T_v	9.61%	7.81%	5.54%	2.03%
Case 2	T_{tr}	24.15%	4.90%	17.53%	2.06%
	T_v	21.73%	21.20%	16.79%	1.86%
Case 3	T_{tr}	26.08%	5.86%	15.54%	1.39%
	T_v	23.36%	25.63%	15.29%	1.35%
Case 4	T_{tr}	10.92%	2.14%	9.38%	1.37%
	T_v	10.24%	1.33%	8.04%	0.44%
Case 5	T_{tr}	16.47%	4.97%	8.58%	0.91%
	T_v	12.43%	7.13%	8.86%	0.47%
Case 6	T_{tr}	15.34%	4.46%	11.78%	2.03%
	T_v	12.15%	5.13%	10.10%	1.10%

findings indicate that the NB effect significantly reduces the molecular dissociation rate compared to the equilibrium dissociation rate over a wide range after the shock.

One of the most significant consequences of this phenomenon is the considerable extension of the thermal nonequilibrium region when considering NB effects, compared to the nonequilibrium region defined by $T_{tr} \neq T_v$. This means that certain flows or areas within the flow field, previously assumed to be in thermal equilibrium and chemical nonequilibrium, are actually in thermochemical nonequilibrium. In our simulations, the impact of thermochemical nonequilibrium is evident through a decelerated dissociation process over longer distances, resulting in elevated fluid temperatures. This can potentially increase surface heat flux. Therefore, accurately considering the NB effect is crucial for predicting and analyzing the behavior of such flows. Table VI presents the percentage differences between the temperatures calculated by Park model and the STS method for each case in this section. The improved model shows significantly smaller average and maximum percentage differences, except for T_v in Cases 2 and 3. The maximum difference in T_v calculated by the improved model for Cases 2 and 3 occurs at the initial stage of the relaxation process ($x \approx 5 \times 10^{-5}$ m). This discrepancy is due to the internal energy relaxation process calculated by the L-T theory rather than the NB correction. Given the low T_v at this stage (approximately 1000 K), a small difference in the T_v value results in a substantial percentage gap. Thus, the maximum percentage difference in T_v in these two cases is not primarily due to NB effects and has a limited impact on the flow. This suggests that the improved model demonstrates significant enhancements in correcting for NB effects in cases where T_{tr} does not exceed 12 000 K and 20 000 K (Cases 3 and 5) after the shock for O_2 and N_2 .

In this section, we compare the relaxation processes after normal shocks in N_2 and O_2 as simulated by different models. The results for both N_2 and O_2 demonstrate that the L-T theory accurately captures the internal energy relaxation process with a reasonable value for the characteristic relaxation time τ . Moreover, the results highlight the persistent nonequilibrium effect caused by the underdistribution of high-energy particles in the system, even after the completion of internal energy relaxation. The Park model and the SGLME model, which do not account for this nonequilibrium effect, exhibit a faster temperature decrease and reach equilibrium significantly earlier than the results obtained from the STS method. In contrast, the improved model, incorporating the NB correction factor ζ , closely aligns with the STS calculations, with minor differences observed only at the beginning of the process and near the completion of internal energy relaxation.

This alignment suggests that the laws governing chemical reaction processes and the influence of NB effects on dissociation rate coefficients, as derived from 0D simulation results, remain applicable

in 1D processes with comparable temperature variations. This also indicates that the improved model, developed based on these principles, not only accurately characterizes the thermochemical nonequilibrium phenomena following a normal shock but also shows potential applicability to other nonequilibrium processes with similar temperature variations.

V. CONCLUSION

The NB effect is predominantly influenced by the equilibrium dissociation degree α_{eq} and the dissociation progress δ . In the nonequilibrium relaxation process triggered by heating, the NB effect demonstrates analogous trends regarding its impact on the dissociation rate of O_2 and N_2 , both of which are homonuclear diatomic molecules. Building upon the identified trends, we have established a fitting formula for the influence factor ζ of the NB effect. During the initial stage of the process, the average value ζ_{av} is employed for ζ . As the process progresses, fitting equations are developed, taking into account the variables α_{eq} and δ . These derived equations aptly portray the influence of the NB effect on the dissociation rate.

Then the improved model was developed by integrating the fitting formula for the NB effect correction factor with the SGLME model. Subsequent validation through simulations of the relaxation process following a normal shock reveals that the improved model adeptly accounts for the impact of thermal nonequilibrium, including nonequilibrium between different internal energy modes and NB effect, on dissociation rates during the heating process. The simulated relaxation process closely matches the calculation results obtained from the STS method and experimental data. This further substantiates that the proposed correction factor ζ accurately represents the influence of the NB effect on dissociation rates.

It is important to note that the improved model is based on similar temperature change processes. The temperature change process experienced by the fluid after the shock wave at the head of the blunt body is similar to the process in our study, which allows for theoretically good results. However, further validation is warranted for processes characterized by different temperature change conditions and flows with substantial diffusion effects between streamlines, such as those occurring within the boundary layer. Additional investigations are necessary to evaluate the applicability of the improved model under such scenarios.

Therefore, the subsequent phase involves validating the improved model in actual flow fields with simulation results derived from the STS method and experimental data. Furthermore, it is essential to consider the properties of different collision pairs and investigate the NB effect on the dissociation rate among air components, as well as pursue the continued development of an improved model specifically tailored to air.

The data that support the findings of this study are available from the corresponding author upon reasonable request.

ACKNOWLEDGMENT

This work was supported by the National Natural Science Foundation of China through Grant No. 11732011.

There are no conflicts of interest.

-
- [1] P. A. Gnoffo, Planetary-entry gas dynamics, *Annu. Rev. Fluid Mech.* **31**, 459 (1999).
 - [2] G. V. Candler, Rate effects in hypersonic flows, *Annu. Rev. Fluid Mech.* **51**, 379 (2019).
 - [3] J. J. Bertin and R. M. Cummings, Critical hypersonic aerothermodynamic phenomena, *Annu. Rev. Fluid Mech.* **38**, 129 (2006).

- [4] L. Landau and E. Teller, On the theory of sound dispersion, *Phys. Z. Sowjetunion* **10**, 34 (1936).
- [5] C. Park, Assessment of a two-temperature kinetic model for dissociating and weakly ionizing nitrogen, *J. Thermophys. Heat Transfer* **2**, 8 (1988).
- [6] C. E. Treanor and P. V. Marrone, Effect of dissociation on the rate of vibrational relaxation, *Phys. Fluids* **5**, 1022 (1962).
- [7] P. V. Marrone and C. E. Treanor, Chemical relaxation with preferential dissociation from excited vibrational levels, *Phys. Fluids* **6**, 1215 (1963).
- [8] C. F. Hansen, Vibrational nonequilibrium effects on diatomic dissociation rates, *AIAA J.* **31**, 2047 (1993).
- [9] A. Sergievskaya, E. Kovach, S. Losev, and N. Kuznetsov, Thermal nonequilibrium models for dissociation and chemical exchange reactions at high temperatures, in *Proceedings of the 31st Thermophysics Conference* (AIAA Press, Reston, VA, 1996), AIAA paper 96-1895.
- [10] A. Sergievskaya, S. Losev, A. Fridman, and S. Macheret, Selecting two-temperature chemical reaction models for nonequilibrium flows, in *Proceedings of the 32nd Thermophysics Conference* (AIAA Press, Reston, VA, 1997), AIAA paper 97-2580.
- [11] P. Hammerling, J. Teare, and B. Kivel, Theory of radiation from luminous shock waves in nitrogen, *Phys. Fluids* **2**, 422 (1959).
- [12] S. Séror, E. Schall, M. C. Druguet, and D. E. Zeitoun, An extension of CVDV model to Zeldovich exchange reactions for hypersonic non-equilibrium air flows, *Shock Waves* **8**, 285 (1998).
- [13] E. Josyula, W. F. Bailey, and C. J. Suchyta III, Dissociation modeling in hypersonic flows using state-to-state kinetics, *J. Thermophys. Heat Transfer* **25**, 34 (2011).
- [14] P. Valentini, T. E. Schwartzentruber, J. D. Bender, and G. V. Candler, Dynamics of nitrogen dissociation from direct molecular simulation, *Phys. Rev. Fluids* **1**, 043402 (2016).
- [15] M. S. Grover, E. Torres, and T. E. Schwartzentruber, Direct molecular simulation of internal energy relaxation and dissociation in oxygen, *Phys. Fluids* **31**, 076107 (2019).
- [16] P. Valentini, T. E. Schwartzentruber, J. D. Bender, I. Nompelis, and G. V. Candler, Direct molecular simulation of nitrogen dissociation based on an *ab initio* potential energy surface, *Phys. Fluids* **27**, 086102 (2015).
- [17] J. G. Kim and I. D. Boyd, State-resolved master equation analysis of thermochemical nonequilibrium of nitrogen, *Chem. Phys.* **415**, 237 (2013).
- [18] K. Neitzel, D. Andrienko, and I. D. Boyd, Aerothermochemical nonequilibrium modeling for oxygen flows, *J. Thermophys. Heat Transfer* **31**, 634 (2017).
- [19] M. S. Grover, E. Josyula, C. J. Suchyta, and K. Vogiatzis, Effect of low and high-fidelity thermochemical models on hypersonic nonequilibrium flows, in *Proceedings of the AIAA Scitech 2019 Forum* (AIAA Press, Reston, VA, 2019), AIAA paper 19-0790.
- [20] D. Ninni, F. Bonelli, G. Colonna, and G. Pascazio, Unsteady behavior and thermochemical non equilibrium effects in hypersonic double-wedge flows, *Acta Astronaut.* **191**, 178 (2022).
- [21] E. Josyula, C. J. Suchyta III, P. Vedula, and J. M. Burt, Multiquantum transitions in oxygen and nitrogen molecules in hypersonic nonequilibrium flows, *J. Thermophys. Heat Transfer* **33**, 378 (2019).
- [22] M. E. Holloway, R. S. Chaudhry, and I. D. Boyd, Assessment of hypersonic double-cone experiments for validation of thermochemistry models, *J. Spacecr. Rockets* **59**, 389 (2022).
- [23] K. N. C. Bray, Vibrational relaxation of anharmonic oscillator molecules: Relaxation under isothermal conditions, *J. Phys. B: At. Mol. Phys.* **1**, 705 (1968).
- [24] K. N. C. Bray, Vibrational relaxation of anharmonic oscillator molecules. II. Non-isothermal conditions, *J. Phys. B: At. Mol. Phys.* **3**, 1515 (1970).
- [25] I. Armenise, M. Capitelli, R. Celiberto, G. Colonna, C. Gorse, and A. Laganà, The effect of $N + N_2$ collisions on the non-equilibrium vibrational distributions of nitrogen under reentry conditions, *Chem. Phys. Lett.* **227**, 157 (1994).
- [26] I. Armenise, M. Capitelli, G. Colonna, and G. Gorse, Nonequilibrium vibrational kinetics in the boundary layer of re-entering bodies, *J. Thermophys. Heat Transfer* **10**, 397 (1996).
- [27] G. Colonna, M. Tuttafesta, M. Capitelli, and D. Giordano, Non-Arrhenius no formation rate in one-dimensional nozzle airflow, *J. Thermophys. Heat Transfer* **13**, 372 (1999).

- [28] G. Colonna, I. Armenise, D. Bruno, and M. Capitelli, Reduction of state-to-state kinetics to macroscopic models in hypersonic flows, *J. Thermophys. Heat Transfer* **20**, 477 (2006).
- [29] D. J. Kewley, Numerical study of anharmonic diatomic relaxation rates in shock waves and nozzles, *J. Phys. B: At. Mol. Phys.* **8**, 2565 (1975).
- [30] G. V. Candler, J. Olejniczak, and B. Harrold, Detailed simulation of nitrogen dissociation in stagnation regions, *Phys. Fluids* **9**, 2108 (1997).
- [31] J. Hao, J. Wang, and C. Lee, State-specific simulation of oxygen vibrational excitation and dissociation behind a normal shock, *Chem. Phys. Lett.* **681**, 69 (2017).
- [32] Q. Hong, X. Wang, Y. Hu, and Q. Sun, Development of a stagnation streamline model for thermochemical nonequilibrium flow, *Phys. Fluids* **32**, 046102 (2020).
- [33] D. Ninni, F. Bonelli, G. Colonna, and G. Pascasio, On the influence of non equilibrium in the free stream conditions of high enthalpy oxygen flows around a double-cone, *Acta Astronaut.* **201**, 247 (2022).
- [34] Y. Liu, M. Vinokur, M. Panesi, and T. Magin, A multi-group maximum entropy model for thermochemical non-equilibrium, in *Proceedings of the 10th AIAA/ASME Joint Thermophysics and Heat Transfer Conference* (AIAA Press, Reston, VA, 2010), AIAA paper 10-4332.
- [35] M. P. Sharma, Y. Liu, and M. Panesi, Coarse-grained modeling of thermochemical nonequilibrium using the multigroup maximum entropy quadratic formulation, *Phys. Rev. E* **101**, 013307 (2020).
- [36] R. L. Macdonald, R. L. Jaffe, D. W. Schwenke, and M. Panesi, Construction of a coarse-grain quasi-classical trajectory method. I. Theory and application to N_2-N_2 system, *J. Chem. Phys.* **148**, 054309 (2018).
- [37] I. Zanardi, S. Venturi, and M. Panesi, Towards efficient simulations of non-equilibrium chemistry in hypersonic flows: A physics-informed neural network framework, in *Proceedings of the AIAA Scitech 2022 Forum* (AIAA Press, Reston, VA, 2022), AIAA paper 22-1639.
- [38] G. Colonna, L. D. Pietanza, and M. Capitelli, Recombination-assisted nitrogen dissociation rates under nonequilibrium conditions, *J. Thermophys. Heat Transfer* **22**, 399 (2008).
- [39] Y. Liu, M. Panesi, A. Sahai, and M. Vinokur, General multi-group macroscopic modeling for thermochemical non-equilibrium gas mixtures, *J. Chem. Phys.* **142**, 134109 (2015).
- [40] E. Josyula and W. F. Bailey, Vibration-dissociation coupling using master equations in nonequilibrium hypersonic blunt-body flow, *J. Thermophys. Heat Transfer* **15**, 157 (2001).
- [41] E. Josyula, W. Bailey, and S. Ruffin, Role of vibration-vibration energy exchanges in nonequilibrium hypersonic flows, in *Proceedings of the 8th AIAA/ASME Joint Thermophysics and Heat Transfer Conference* (AIAA Press, Reston, VA, 2002), AIAA paper 02-3220.
- [42] N. Singh and T. Schwartzentruber, Consistent kinetic-continuum dissociation model. I. Kinetic formulation, *J. Chem. Phys.* **152**, 224302 (2020).
- [43] N. Singh and T. Schwartzentruber, Consistent kinetic-continuum dissociation model. II. Continuum formulation and verification, *J. Chem. Phys.* **152**, 224303 (2020).
- [44] T. K. Mankodi and R. S. Myong, Quasi-classical trajectory-based non-equilibrium chemical reaction models for hypersonic air flows, *Phys. Fluids* **31**, 106102 (2019).
- [45] R. S. Chaudhry and G. V. Candler, Statistical analyses of quasiclassical trajectory data for air dissociation, in *Proceedings of the AIAA Scitech 2019 Forum* (AIAA Press, Reston, VA, 2019), AIAA paper 19-0789.
- [46] G. D. Billing, Semiclassical calculation of cross sections for vibration-rotation energy transfer in HF-HF collisions, *J. Chem. Phys.* **84**, 2593 (1986).
- [47] R. S. Chaudhry, I. D. Boyd, and G. V. Candler, Vehicle-scale simulations of hypersonic flows using the MMT chemical kinetics model, in *Proceedings of the AIAA Aviation 2020 Forum* (AIAA Press, Reston, VA, 2020), AIAA paper 20-3272.
- [48] R. S. Chaudhry, I. D. Boyd, E. Torres, T. E. Schwartzentruber, and G. V. Candler, Implementation of a chemical kinetics model for hypersonic flows in air for high-performance CFD, in *Proceedings of the AIAA Scitech 2020 Forum* (AIAA Press, Reston, VA, 2020), AIAA paper 20-2191.
- [49] I. Zanardi, S. Venturi, A. Munafò, and M. Panesi, Towards efficient simulations of non-equilibrium chemistry in hypersonic flows: Neural operator-enhanced 1-d shock simulations, in *Proceedings of the AIAA Scitech 2023 Forum* (AIAA Press, Reston, VA, 2023), AIAA paper 23-1202.

- [50] M. L. Da Silva, V. Guerra, and J. Loureiro, State-resolved dissociation rates for extremely nonequilibrium atmospheric entries, *J. Thermophys. Heat Transfer* **21**, 40 (2007).
- [51] C. E. Treanor, Vibrational energy transfer in high-energy collisions, *J. Chem. Phys.* **43**, 532 (1965).
- [52] I. V. Adamovich, S. O. Macheret, J. W. Rich, and C. E. Treanor, Vibrational energy transfer rates using a forced harmonic oscillator model, *J. Thermophys. Heat Transfer* **12**, 57 (1998).
- [53] A. J. Fangman and D. A. Andrienko, Vibrational-specific model of simultaneous N₂-N and N₂-N₂ relaxation under postshock conditions, *J. Thermophys. Heat Transfer* **36**, 1 (2022).
- [54] R. Xiong, Y. Han, and W. Cao, Vibration non-Boltzmann effect on dissociation rate of oxygen, *Phys. Chem. Chem. Phys.* **25**, 19073 (2023).
- [55] T. E. Schwartztruber, M. S. Grover, and P. Valentini, Direct molecular simulation of nonequilibrium dilute gases, *J. Thermophys. Heat Transfer* **32**, 892 (2018).
- [56] L. Ibraguimova, A. Sergievskaya, V. Y. Levashov, O. Shatalov, Y. V. Tunik, and I. Zabelinskii, Investigation of oxygen dissociation and vibrational relaxation at temperatures 4000–10 800 K, *J. Chem. Phys.* **139**, 034317 (2013).
- [57] C. Park, Assessment of two-temperature kinetic model for ionizing air, *J. Thermophys. Heat Transfer* **3**, 233 (1989).
- [58] J. Hao and C.-Y. Wen, Maximum entropy modeling of oxygen vibrational excitation and dissociation, *Phys. Rev. Fluids* **4**, 053401 (2019).
- [59] X. Wang, Q. Hong, Y. Hu, and Q. Sun, On the accuracy of two-temperature models for hypersonic nonequilibrium flow, *Acta Mech. Sin.* **39**, 122193 (2023).